DE GRUYTER OPEN

Journal of ELECTRICAL ENGINEERING, VOL 68 (2017), NO7, 24–30

Nanocrystalline proprieties of TiO_2 thin film deposited by ultrasonic spray pulverization as an anti-reflection coating for solar cells applications

Samira Sali[*,], Salim Kermadi[*], Lyes Zougar[*], Bouthina Benzaoui[**], Nadia Saoula[***], Khadija Mahdid[*], Fatiha Aitameur[*], Messaoud Boumaour[*]**

Titanium oxide (TiO_2) films have been synthesized on quartz, silicon and textured silicon substrates by chemical ultrasonic spray deposition. The textured silicon substrate was carried out using Na_2CO_3 solution. The sample surface exhibits uniform pyramids with an average height of 5μm . In this paper, particular attention is given to the TiO_2 films prepared by spray ultrasonic system using Tetra iso-Propoxide Orthotitanate Titanium (TPOT) as a precursor. The solutions were sprayed onto substrates heated at various temperatures 350 - 550 °C . The properties of films as a function of temperature parameter were investigated using structural and optical analysis. According to XRD, FTIR and Micro- Raman spectroscopies, the anatase phase was found and exhibits nanograins of 9 to 15 nm in size. The indirect and direct bad gap were found to increase by increasing substrate temperature due to the decreasing of nanograins size and were estimated to be around 3.28 and 3.38 eV. A transmittance higher than 80% was found. This paper reports on anti- reflection coating application of TiO2 layers due to its good transparency and appropriate refractive index varies between 2.19 - 2.40 at $\lambda = 632.8$ nm as a function of temperature determined by UVVisNIR spectrophotometer and Ellipsometry. To achieve optimum anti-reflection characteristics different anti-reflection designs were experimentally examined with polished and textured substrates. The average reflectance of the polished silicon used in this study is 39%, with TiO_2 it decreases to 9%. The textured surface reduces the average reflectance of silicon to be around 14% and it decreases dramatically to 5% after deposition of a single layer of TiO_2 as an anti-reflection coating. The gain in density of the short-circuit photocurrent assigned to the reduction of reflection losses up to 44% and 58% were predicted with TiO_2 single-coating in polished and textured silicon substrates respectively.

K e y w o r d s: TiO_2, spray ultrasonic, textured silicon, anti-reflection coating

1 Introduction

Promising application such as anti-reflection coatings (ARC) for solar cells, which is an area where research is still very active to minimize reflectance surface and therefore directly improve the short-circuit current of the device (and final performance conversion) [1-3]. The performance of ARC for solar cells is distinguished by various aspects: The control of refractive index (n) of coatings is the key point to achieve excellent anti-reflection performance, the large transmittance for the broad solar spectrum (generally, in the range from 300 to 1200 nm) and the front surface structure in solar cells, which complicates the designs a lot. Various ARC single and double layers have been widely studied, such as ZnO [4], SiN [5], ITO [6], SiO_2/SiN [7], MgF_2/ZnS [8], SiO_2/Na_2CO_3[9], Na_2CO_3[10] and Al_2O_3/Na_2CO_3[11] coatings. Increasing the efficiency of photovoltaic devices by reducing the reflectance on their front surface has been a widely studied issue in the last few decades. Traditionally, bulk silicon solar cells have been optimized by combining anti-reflective coatings (such as Si_2N_4: H) and surface texturization [12].

In this paper an attention is given to TiO_2 thin layer for anti-reflection coating application. Due to its properties, it is non-toxic, stable with a large band gap of about 3.2 eV and 3 eV for anatase and rutile TiO_2 respectively, it is a material with good transparency and high refractive index ($n = 2.52$) [13].

TiO_2 has a large variety of potential application as gas sensors, planar waveguide, photocatalyst, ceramic membrane anti-reflective coating in solar cells [14-17]. Various deposition techniques have been widely used to produce TiO_2 thin films. However, the most intensively studied techniques include RF magnetron sputtering [18], chemical vapor deposition (CVD) [19], the solgel method [20], thermal evaporation [21] and the spray pyrolysis [22, 23] among others. In this study, ultrasonic spray technique is used because of its easy deposition and low cost. In comparison with other chemical deposition techniques,

* CRTSE - Division DDCS, 02 Bd Dr. Frantz Fanon BP, 140, les 07 Merveilles, 16038, Algiers, Algeria, samira$_s$ali@yahoo.fr, ** Houari Boumediene University, faculty of physics, BP 32 El Alia Algiers, Algeria, *** Centre de Développement des Technologies Avancées, BP 17 Baba Hassen, Alger, Algrie

DOI: 10.1515/jee-2017–0051, Print (till 2015) ISSN 1335-3632, On-line ISSN 1339-309X

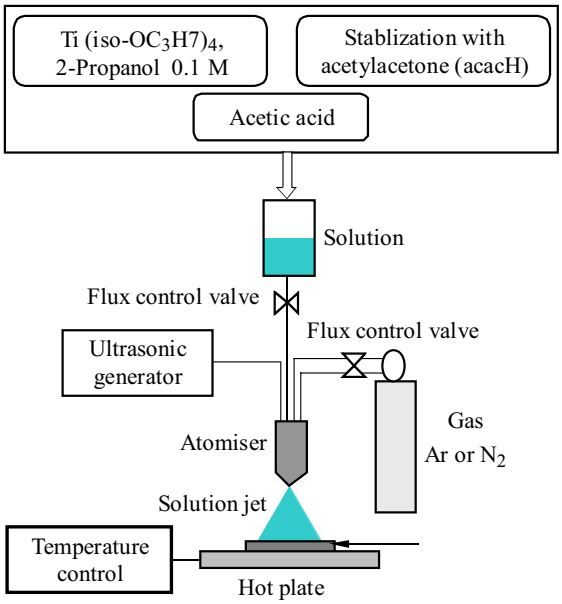

Fig. 1. The experimental set-up

spray pyrolysis has several advantages such as high purity, excellent control of chemical uniformity and stoichiometry in multi-component systems. The other advantage of the spray pyrolysis method is the easy adaptation for the production of large-area films. With our deposition system, uniform TiO_2 layers can be deposited on an area of 100 cm^2.

In this work, TiO_2 thin films were deposited ont quartz; polished silicon and combining with textured su face silicon substrates. Optical studies were carried out t analyze the influence of the substrate temperature on th nanostructural features of the TiO_2 as an anti-reflectic coating using several methods.

2 Experimental details

TiO_2 films were obtained by the spray ultrasonic m thod. The starting solution was prepared by dissolvi Tetra iso-Propoxide Orthotitanate Titanium (TPOT) i 2-propanol (i-PrOH) and Acetylacetone (AcAc). The co centration of TPOT was fixed at 0.1 mole/l and th TPOT: AcAc molar ratio of 1:1.5. The experimental se up Na_2CO_3thin film preparation is shown in Fig. 1. The layers are deposited onto textured c-Si (100), polishe surface c-Si (100) and quartz substrates. In this process, nitrogen was used as the carrier gas. The spray rate and deposition time were fixed at 8 ml/min and 5 min, respectively. The solutions were sprayed onto heated substrates at various temperatures 350 to 550 °C, for the temperature less than 420 °C, a powder of $Na_2CO_3$is obtained without a good adherence. Also, when a temperature is higher than *geq* 420 °C, a blue layer onto polished silicon substrate with very high adherence is elaborated and confirmed by different durability and stability tests. Concerning the textured Si substrate, the solution used is based on $Na_2CO_3$and the image of textured surface covered with a multitude pyramids having an average height of 5μm are shown in Fig. 2.

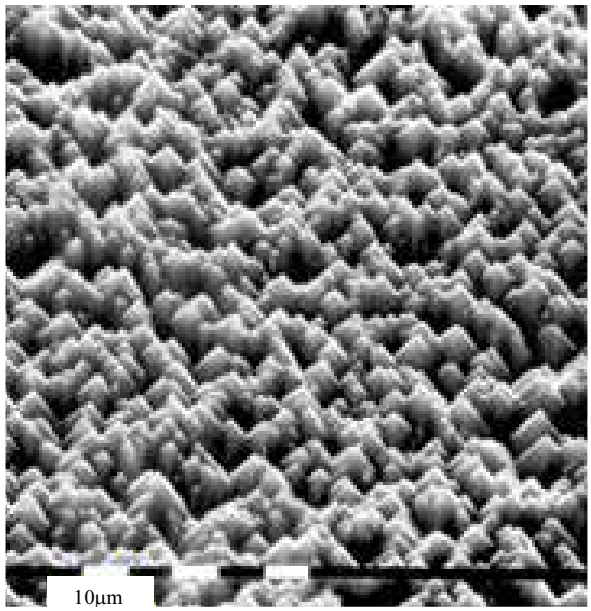

Fig. 2. Plan view SEM image of textured silicon etched in an anisotropic solution of TiO_2

The structure of the TiO_2 thin films was analyzed by X-ray diffraction (XRD) measurement (Bruker D8 Advance from CDTA, Algiers) using Cu Kα radiation (λ = 0.154 nm) in the 2θ configuration and micro-Raman spectroscopy with a Jobin-Yvon ARAMIS micro-Raman spectrometer working in back-scattering configuration. The

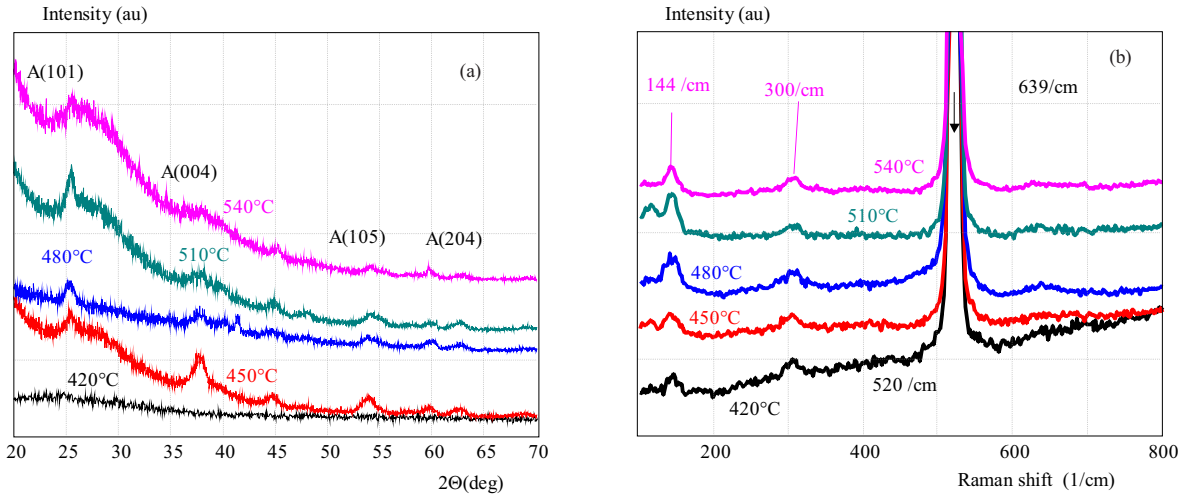

Fig. 3. (a) – XRD patterns, and (b) – Raman shift spectra of TiO_2 films deposited at different substrate temperature

excitation line at 633 nm was provided by Laser He/Ne, 17 mW. Fourier transforms infrared (FTIR) absorption measurements were carried out with a Thermo Nicolet NEXUS 670 spectrometer (from CRTSE, Algiers). Reflectance and transmittance measurements were carried out with double beam Cary 500 UVVisNIR spectrophotometer (from CRTSE, Algiers) equipped with an integrating sphere. The transmittance data were recorded on quartz substrate which its effect was subtracted using identical uncoated quartz as a blank in the double beam. The reflectance data was recorded on silicon using the integrating sphere at the near-normal incident angle of 8 deg. The refractive index of the films nm was determined with ELX-02C monochromatic ellipsometry at $\lambda = 632.8$ nm.

3 Results and discussion

3.1 Structural characterization: XRD and Raman spectroscopy

Figure 3(a) shows the XRD patterns of TiO_2 films elaborated at different substrate temperature on quartz substrates. The all spectrum exhibit peaks corresponding to the anatase phase of TiO_2 (JCPDS No.21-1272). The mean crystallite size of TiO_2 films was calculated using the Scherrer's formula

$$D = \frac{0.9\lambda}{\beta \cos\theta},$$

where λ, θ and β are the X-ray wavelength (1.5418 Å), Bragg diffraction angle and full width at half maximum FWHM in radians of the (101) diffraction peak, respectively. The nanograins size decreases from 15 to 9 when substrate temperature increases.

The films were also analyzed by micro-Raman spectroscopy, Fig. 3(b). All spectra of TiO_2 films displays the main peak at 144 cm^{-1} characteristic of the mode E_g of the anatase phase and a peak at 639 cm^{-1} assigned to this phase of TiO_2 [24], other peaks than those due to the Si substrate at 520 cm^{-1}, 300 cm^{-1} are observed. It can be observed in these spectra that the band enlargement of 144 cm^{-1} peak varies as a function of substrate temperature, this is it can be attributed to the variation of nanocrystals sizes of TiO_2 [25-28], this result is in good accord with XRD measurements.

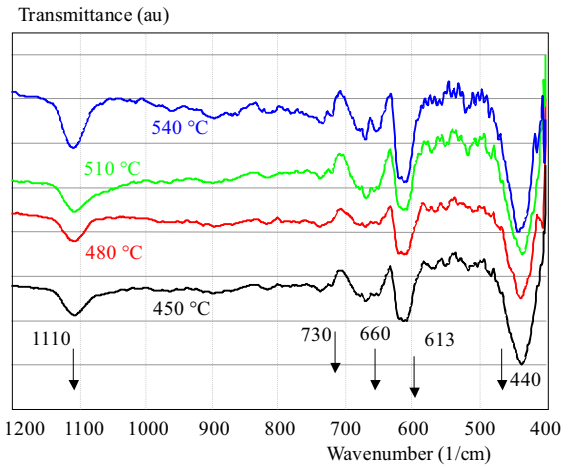

Fig. 4. Infrared spectra of TiO_2 films deposited at different substrate temperature

3.2 Structural characterization: FTIR analysis

The infrared spectra of TiO_2 films elaborated at different substrate temperature before annealing have been recorded to study the vibrational bands present in the system as projected in Fig.4. Generally, the infrared spectra give information about functional groups present in a system, the molecular geometry, and inter or intramolecular interactions. A large broad absorption peak at 3150 cm^{-1} is attributed to the OH (hydroxyl) group. All the spectra show a peak at 613 cm^{-1} which is associated to SiSi vibrations of the silicon substrate [29]. The strong peak at 1100 cm^{-1} and weak peaks at 812 and 463 cm^{-1} are assigned to SiOSi vibrations in pure SiO_2 [30,31]. The peaks centered at 440 cm^{-1}, 660 cm^{-1} and 730 cm^{-1} observed it can be assigned to Ti-O-Ti vibrations, [32].

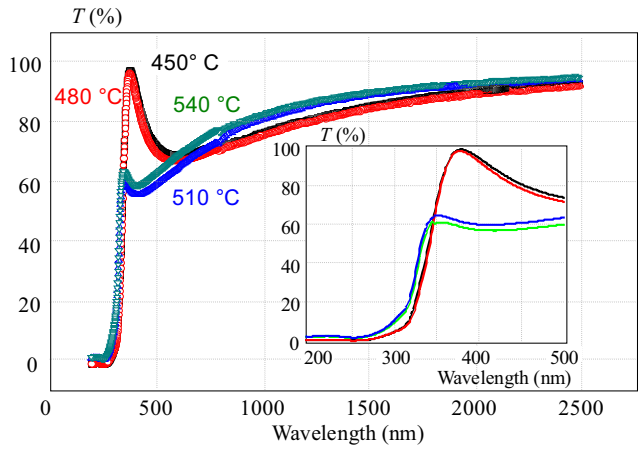

Fig. 5. Transmittance spectra of TiO_2 films deposited on quartz substrate at different temperature

3.3 Optical characterization: Transmission and optical gap

Figure 5 shows the transmission spectra for TiO_2 layers deposited on quartz substrates. All the films studied were uniform and transparent to the naked eye.

The transmittance spectra in the range of 400 1200 nm revealed that all films exhibit high transmittance of the order 85%. From the transmittance spectra, we can conclude that the samples elaborated at substrate temperature less than 510 °C are more transparent, this result could be attributed to the loss scattering due to the high crystalline size of the grain and the high roughness of the surface. According Tauc formula [33], the indirect band gap was determined from the transmittance spectra

$$\alpha(E) = A(E - E_g)^m, \tag{1}$$

where $E = h\nu$ is the photon energy and E_g is the band energy, A is a constant and m is an index that characterizes the optical absorption, is equal to 2 for indirect allowed transition and to 0.5 for direct allowed transition. At shorter wavelengths close to the optical band gap, may be deduced

$$\alpha = \frac{1}{d} \ln \frac{1}{T}. \tag{2}$$

From the plots $(\alpha E)^{1/2}$ versus E in Fig. 6, the indirect and direct bad gap were found to increase by increasing substrate temperature, Fig. 7. This band gap blue shift value could be attributed to the decrease of the crystallite size [34].

3.4 Optical characterization: Ellipsometry and anti-reflection proprieties

Due to the high refractive index of silicon ($n = 3.9$), an important optical loss occurs on its surface and about 39% of the total incoming light is reflected (for silicon substrate used in this work the average reflectance is 39.24%, the textured Si reduced light reflection to 14.25% for wavelengths ranging from 400 to 1000 nm compared with the reflectivity of the c-Si sample Fig. 8(a). For solar cells, this behavior should be reduced as maximum as possible [34]. Therefore, its Surface should be coated by a dielectric material exhibiting high transparency and low absorption. All TiO_2 films exhibits comparable thicknesses of about 74 nm and the refractive index varies between 2.19 and 2.39 as a function of temperature. A TiO_2 single-layer anti-reflective coating is deposited onto polished silicon substrate at different substrate temperature. The reflectance spectra are shown in Figure 8(b). In order to determine the effectiveness of an AR coating, the solar averaged reflectance was calculated by averaging the reflectance data overran AM1.5 solar photons spectral distribution. The average reflectivity was calculated and it decreases the reflectance of Si to 9 - 14% in [400 - 1000] as a function of substrate temperature. The textured surface was found to be around 14% and it decreases dramatically to 5.2% and after deposition of a single layer of TiO_2 as an anti-reflection coating Fig. 8(c).

In order to determine the effectiveness of an AR coating, the solar averaged reflectance was calculated by averaging the reflectance data over an AM1.5 solar photon spectral distribution $f(\lambda)$. The average reflectivity was calculated using the following equation [34]

$$R = \frac{\int f(\lambda) R(\lambda) \mathrm{d}\lambda}{\int f(\lambda) \mathrm{d}\lambda} \tag{3}$$

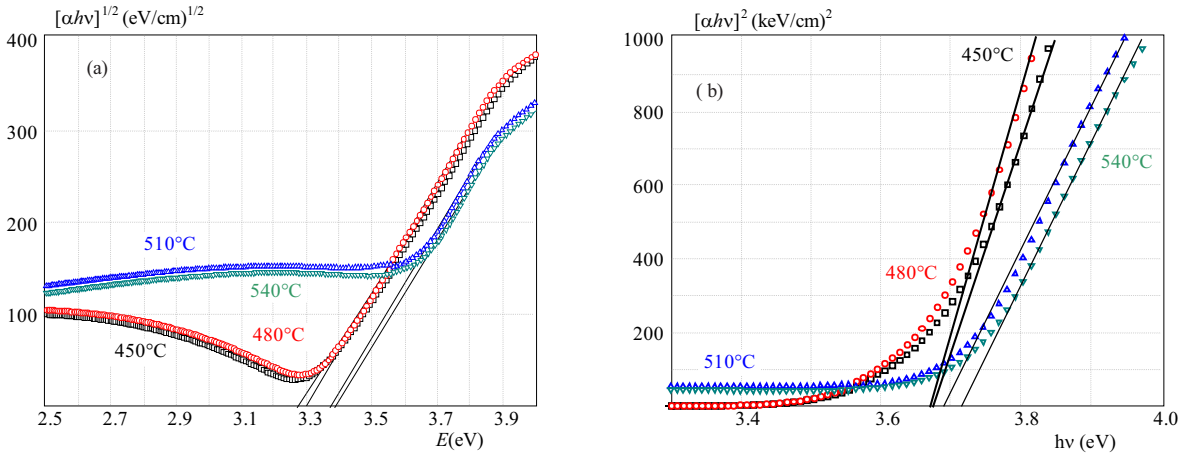

Fig. 6. Plots $(\alpha E)^{1/2}$ versus E of indirect and direct transition for TiO_2 thin films at different substrate temperature

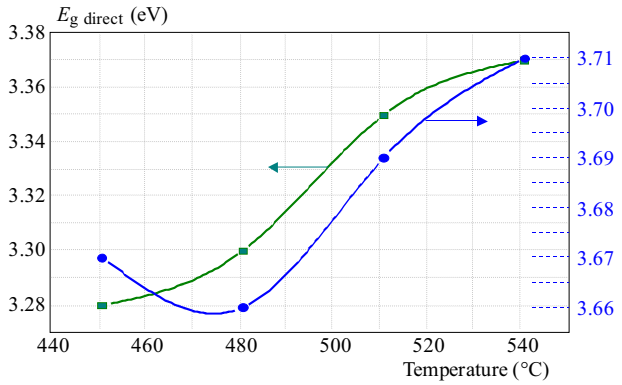

Fig. 7. Direct and indirect optical band gap as a function of substrate temperature

where $R(\lambda)$ is the reflectivity as a function wavelength and $f(\lambda)$ is the incident AM1.5 photon flux as a function wavelength.

The limits of integration were set equal to the active range of silicon which extends from 320 to 1120 nm. The average reflectance values calculated in this way represent the fractional amount of solar photons within the active range for silicon that are reflected by the cell. Since silicon is opaque over this wavelength range, one minus the average reflectance gives the fraction of photons that are absorbed by the cell. The R_{avr} between 400 and 1000 nm is plotted as a function of substrate temperature in Figure 9(a),(b) for polished and textured silicon. The lowest values of 9.75% and 6.25% are obtained in the range of 450-480 °C for polished and textured silicon, respectively.

The impact of the anti-reflection coating in solar cells can be expressed by the ration $\Delta J_{sc}/J_{sc}$ in equation below, which describes the gain in the density of the short-circuit photocurrent J_{sc} assigned only to the reduction of reflection losses

$$\frac{\Delta J}{J_{sc0}} = \frac{J_{sc} - J_{sc0}}{J_{sc0}} \tag{4}$$

where J_{sc} is with, while J_{sc0} is without ARC, and where

$$J_{sc} = \int f(\lambda) IQE(\lambda) R(\lambda) \mathrm{d}\lambda \tag{5}$$

with q being the electron charge, $f(\lambda)$ - the AM1.5 solar photon spectral distribution [6], $R(\lambda)$ is the reflectance, and $IQE(\lambda)$ the internal quantum efficiency of the solar cell. Referring to an ideal cell with $IQE = 1$ and integrating from $\lambda_1 = 400$ to $\lambda_2 = 1000$ nm, J_{sc} increases from 21.64 mA/cm^2 for uncoated solar cell ($R_{avr} = 39.24\%$) up to 31.13 mA/cm^2 for a textured surface ($R_{avr} = 14.27\%$) leading to 43.85% gain, whereas by using a single layer of TiO_2 on a textured surface, which reveals an increases in J_{sc} value to 34.17 mA/cm^2 leading to 58.02% gain. Table 1 summarizes the impact of the anti-reflection coating in solar cells.

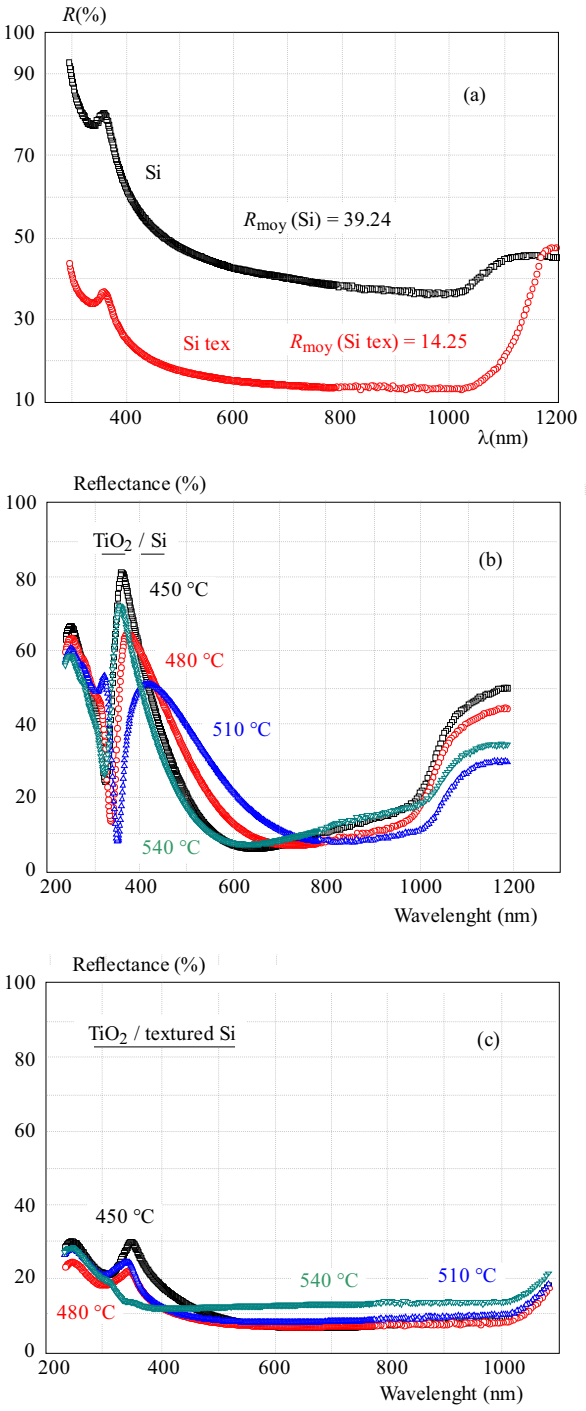

Fig. 8. Reflectance spectra of TiO_2 films deposited: (a) – of polished and textured silicon substrate, (b) – of polished silicon substrate at different substrate temperature, (c) – of textured silicon substrate at different substrate temperature

Table 1. Peak position after deconvolution of absorption 950 -1250 cm^{-1}

T_{sub} :	450 °C	480 °C
	$\frac{\Delta J}{J_{sc0}}$ (%)	
TiO_2 /Si	44.45	40.52
Si texturized/Si	43.85	-
TiO_2 /Si texturized/Si	56.65	58.02

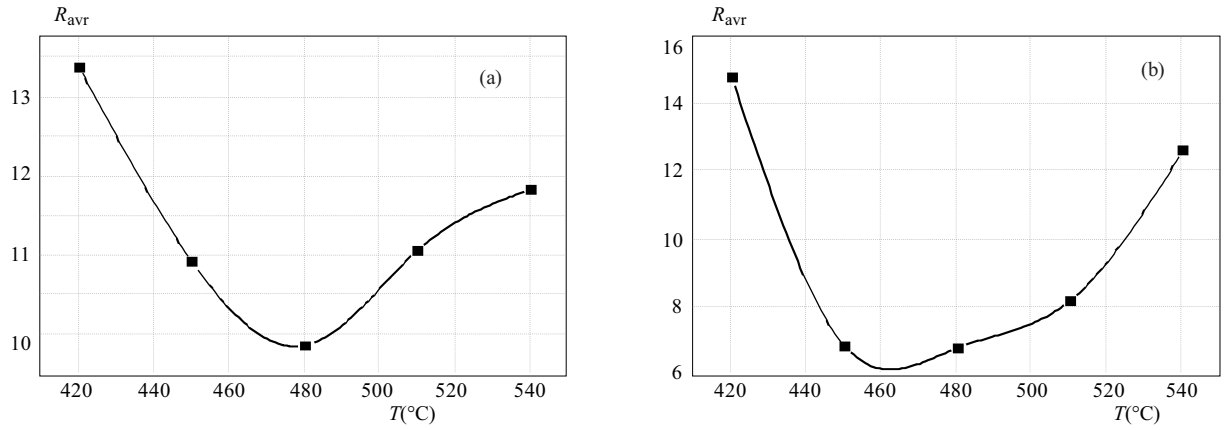

Fig. 9. R_{avr} between 400 and 1000 nm is plotted as a function of substrate temperature for TiO_2 : (a) – polished silicon, and (b) – textured silicon

4 Conclusions

In summary, TiO_2 thin films with good adherence chemical and mechanical stabilities were successfully synthesized on quartz, virgin silicon and textured silicon substrates by chemical ultrasonic spray deposition using Tetra iso-Propoxide Orthotitanate Titanium (TPOT) as a precursor. According to structural characterization the anatase phase was found and the TiO_2 films exhibit nanograins size which decreases from 15 to 9 nm with increasing temperature. The optical band gap was estimated to be around 3.28 - 3.38 eV. In addition, the films exhibit high transparency films (transmittance over 80%) with very low absorption in UVvisible spectral range. The paper reports on anti-reflection coating application of TiO_2 films due to its good transparency and appropriate refractive index (2.19 - 2.39) determined by UVvisibleNIR spectrophotometer and Ellipsometry. The average reflectance of the polished silicon is 39%, which decreases to reach 9.75% with TiO_2. The textured surface was found to be around 14.27% and decreases dramatically when using a single layer of TiO_2 to reach 5.2% advantages for an anti-reflection application, leading to 58% of gain in density of the short-circuit photocurrent assigned to the reduction of reflection. Finally, it has been found that ultrasonic process and combination of TiO_2 with textured substrate could be a viable option and an effective low-cost route, for producing coatings with controllable thicknesses and graded refractive index nanomaterial, exhibiting high purity and high optical qualities required for numerous optical applications such as the anti-reflective coating to improve the efficiency solar cells.

Acknowledgements

This work was supported by Funds National Research (DG-RSDT/MESRS, Algeria).

References

[1] K. Choi, S. H. Park, Y. M. Song, Y. T. Lee, C. K. Hwangbo, H. Yang and H. S. Lee, "Nano-tailoring the surface structure for the monolithic high-performance anti-reflection polymer film", *Adv. Mater*, vol. 22 (2010) 3713-3718.

[2] J. H. Son, J. U. Kim, Y. H. Song, B. J. Kim, C. J. Ryu and J. L. Lee, "Design rule of nanostructures light-emitting diodes for complete elimination of total internal reflection", *Adv. Mater.*, vol. 24 (2012) 2259-2262.

[3] Dezeng Li, Dongyun Wan, Xiaolong Zhu, Yaoming Wang, Zhen Han, Shuangshuang Han, Yongkui Shan and Fuqiang Huang, "Broadband anti-reflection TiO_2 - SiO_2 stack coatings with refractive-index-grade structure and their applications to Cu(In, Ga)Se_2 solar cells", *Solar Energy Materials & Solar Cells*, vol. 130(2014) 505-512.

[4] S. Sali, M. Boumaour, M. Kechouane, S. Kermadi and F. Aitamar, "Nanocrystalline ZnO film deposited by ultrasonic spray on textured silicon substrate as an anti-reflection coating layer", *Physica B*, vol. 407 (2012) 2626-2631.

[5] Yanyan Wang, Biao Shao, Zhen Zhang, Lanjian Zhuge, Xuemei Wu and Ruiying Zhang, "Broadband and omnidirectional anti-reflection of Si nanocone structures cladded by SiN film for Si thin film solar cells", *Optics Communications*, vol. 316 (2014) 37-41.

[6] W. C. Tien and A. K. Chu, "Double-layer ITO anti-reflection electrodes fabricated at low temperature", *Solar Energy Materials and Solar Cells*, vol. 100 (2012) 258-262.

[7] A. Lennie, H. Abdullah, Z. M. Shila, and M. A. Hannan, "Modeling and simulation of SiO2/Si3N4 as anti-reflecting coating for silicon solar cell by using Silvaco Software", *World Applied Sciences Journal*, vol. 11(7) (2010) 786-790.

[8] S. M, Jung, Y.H. Kim, S. I. Kim and S. I. Yoo, "Design and fabrication of multi-layer anti-reflection coating for III-V solar cell", *Current Applied Physics*, vol. 11 (2011) 538-541.

[9] S. Kermadi, N. Agoudjil, S. Sali, M. Boumaour, S. Bourgeois and M. C. Marco de-Lucas, "Sol-gel synthesis of xTiO_2 (100-x) SiO_2 nanocomposite thin films: Structure, optical and anti-reflection properties", *Thin Solid Films*, vol. 564 (2014) 170-178.

[10] Zhaoyong Wang, Ning Yao and Xing Hu, "Single material TiO_2 double layers anti-reflection coating with photocatalytic property prepared by magnetron sputtering technique", *Vacuum*, vol. 108 (2014) 20.

[11] Dong Sing, Wuu, Che Chun, Lin, Chao Nan, Chen, Hong Hsiu Lee and Jung Jie Huang, "Properties of double-layer Al2O3/TiO_2 anti-reflection coatings by liquid phase deposition", *Thin Solid Films*, Press, Corrected Proof, Available online 29 January 2015.

[12] M. F. Saenger, J. Sun, M. Schdel, J. Hilfiker, M. Schubert and J. A. Woollam, "Spectroscopic ellipsometry characterization of SiNx anti-reflection films on textured multicrystalline and monocrystalline silicon solar cells", *Thin Solid Film*, vol. 518, no. 7 (2010) 1830.

[13] X. T. Zhang, A. Jin, M. Fujishima, A. V. Emeline and T. Murakami, "Double-layered TiO_2 /SiO2 nanostructured films with self-cleaning and anti-reflective properties", *J Phys Chem B*, vol. 110 (2006) 25142e8.

[14] CH. Ashok and K. Venkateswara-Rao, "ZnO/TiO_2 nanocomposite rods synthesized by microwave-assisted method for humidity sensor application", *Superlattices and Microstructures*, 76 (2014), 46.

[15] S. Kumbhar, V. P. Kothavale, A. V. Moholkar, K. Y. Rajpure and C. H. Bhosale, "Photoelectrocatalytic degradation of benzoic acid using sprayed TiO_2 thin films", *Ceramics International*, vol. 41, no. 2, Part A, (2015), 2202.

[16] M. O. Abou-Helal and W. T. Seeber, *Appl. Surf. Sci.*, vol. 195 (2002) 53.

[17] L. Castaneda, J. C. Alonso, A. Ortiz, E. Andrade, J. M. Saniger and J. G. Banuelos, *Mater. Chem. Phys.*, vol. 77 (2002) 938.

[18] S. Ohno, D. Sato, M. Kon, M. Yoshikawa, K. Suzuki, P. Frach and Y. Shigesato, *Thin Solid Films*, vol. 445 (2003) 207.

[19] K. Ikeue, H. Yamashita and M. Anpo, *Chem. Lett.*, vol. 28 (1999) 1135.

[20] S. Kermadi, N. Agoudjil, S. Sali, L. Zougar, M. Boumaour, L. Broch, A. En Naciri and F. Placido, "Microstructure and optical dispersion characterization of nanocomposite sol-gel TiO_2 -SiO_2 thin films with different compositions", *Spectrochimica Acta Part A Molecular and Biomolecular Spectroscopy* (2015), http://dx.doi.org/10.1016/j.saa.2015.02.110.

[21] H. K. Pulker, G. Paesold and E. Ritter, *Appl. Opt.*, vol. 15 (1976) 2986.

[22] L. Kavan and M. Grätzel, *Electrochim. Acta*, vol. 40 (1995) 643.

[23] I. Oja Acika, V. Kiisk, M. Krunks, I. Sildos, A. Junolainen, M. Danilson, A. Mere and V. Mikli, "Characterisation of samarium and nitrogen co-doped TiO_2 films prepared by chemical spray pyrolysis", *Applied Surface Science*, vol. 261 (2012) 735.

[24] S. Boukrouh, R. Bensaha, S. Bourgeois, E. Finot and M. C. Marco de Lucas, "Reactive direct current magnetron sputtered TiO_2 thin films with amorphous to crystalline structures", *Thin Solid Films*, vol. 516 (2008) 6353.

[25] S. Kelly, F. H. Pollak and M. Tomkiewicz, "Raman spectroscopy as a morphological probe for TiO_2 aerogels", *Journal of Physical Chemistry B*, vol. 101 (1997) 2730.

[26] W. Ma, Z. Lu and M. Zhang, "Investigation of structural transformations nanophase titanium dioxide by Raman spectroscopy", *Applied Physics A, Materials Science and Processing*, vol. 66 (1998) 621.

[27] D. Bersani, P. P. Lottici and X. Z. Ding, "Phonon confinement effects the Raman scattering by TiO_2 nanocrystals", *Applied Physics Letters*, vol. 72(1), 73 (1998).

[28] A. LiBassi, D. Cattaneo, V. Russo, C. E. Bottani, E. Barborini, T. Mazza, P. Piseri, P. Milani, F. O. Ernst and K. Wegner, "Raman spectroscopy characterization of titania nanoparticles produced by flame pyrolysis: The influence of size and stoichiometry", *Journal of Applied Physics*, vol. 98 (2005) 074305 1.

[29] G. Sahu, H. P. Lenka, D. P. Mahapatra, B. Rout and F. D. McDaniel, "Narrow band UV emission from direct bandgap Si nanoclusters embedded bulk Si", *J. Phys. Condens. Matter*, vol. 22 (2010) (072203, 5.

[30] X. M. Du and R. M. Almeida, "Effects of thermal treatment on the structure and properties of SiO2-TiO_2 gel films on silicon substrates", *J. Sol-Gel Sci. Technol.*, vol. 8 (1997) 377.

[31] C. S. Wu, "Synthesis of polyethylene-octene elastomer/SiO2-TiO_2 nanocomposites viain situ polymerization: properties and characterization of the hybrid", *J. Polym. Sci. A Polym. Chem.*, vol. 43 (2005) 1690.

[32] N. Arconada, A. Duran, S. Suarez, R. Portela, J. M. Coronado, B. Sanchez and Y. Castro, "Synthesis and photocatalytic properties of dense and porous TiO_2 - anatase thin films prepared by sol-gel", *Appl. Catal. B Environ.*, vol. 86 (2009) 1.

[33] J. Tauc, *Amorphous and Liquid Semiconductors*, Plenum Press, NewYork, 1974.

[34] I. G. Kavakli and K. Kantarli, "Single and double-layer antireflection coatings on silicon", *Turk. J. Phys.*, vol. 26 (2002) 349.

Received 23 April 2017